

Numerical analysis of applied magnetic field dependence in Malmberg-Penning Trap for compact simulator of energy driver in heavy ion fusion

T Sato¹, Y Park², Y Soga², K Takahashi¹, T Sasaki¹, T Kikuchi¹, and Nob.Harada¹

¹Nagaoka University of Technology, Nagaoka, Niigata, Japan

²Kanazawa University, Kanazawa, Ishikawa, Japan

tomohiro_sato@stn.nagaokaut.ac.jp

Abstract. To simulate a pulse compression process of space charge dominated beams in heavy ion fusion, we have demonstrated a multi-particle numerical simulation as an equivalent beam using the Malmberg-Penning trap device. The results show that both transverse and longitudinal velocities as a function of external magnetic field strength are increasing during the longitudinal compression. The influence of space-charge effect, which is related to the external magnetic field, was observed as the increase of high velocity particles at the weak external magnetic field.

1. Introduction

An energy driver development is a key issue for inertial fusion energy. In inertial confinement fusion (ICF) driven by heavy ion beams (HIB), several system configurations have been considered [1-4]. These systems at the final stage of the particle accelerator system require the high-current HIB [4]. To obtain the high-current HIB, a beam bunch should be compressed more than 10 times in the longitudinal direction [5-10]. By the pulse compression in the longitudinal direction, HIB undergoes a transition from an emittance-dominated regime to a space-charge-dominated regime. Because the required parameters for HIB in ICF are far from that of the conventional beams, the beam behaviors, which is in the condition dominated by the space-charge effect, should be researched well for the energy driver development.

Instead of the HIB, the equivalent beam dynamics can be simulated with a compact experimental apparatus using the electron beam, which is in the condition dominated by the space-charge effect. For this reason, the beam dynamics simulation in the pulse compression of the HIB has been demonstrated using the Malmberg-Penning trap device [11]. Simulating beam parameters in a compact experimental apparatus using the electron beam are evaluated by the tune depression, which is an index for space charge strength in the beam bunch. In this index, the space charge strength is evaluated as the dependence on external magnetic field strength and number density on the space-charge effect [12].

In this study, we have numerically investigated the dependence on external magnetic field for the beam dynamics in the Malmberg-Penning trap device [13] as the compact simulator of HIB. For this purpose, the multi-particle numerical simulation based on particle-particle method is performed the



compression process in different external magnetic field conditions, and we analyzed real and phase space distributions.

2. Malmberg-Penning trap device

A Malmberg-Penning trap device [13] is a confinement device of electron cloud, and can investigate non-neutral plasmas on controlling the density distribution. The parameters of this device are maximum external magnetic field of 0.1 T along the axial direction, and the voltage of well shaped potential barriers is -100 V at both axial ends. The electron motions are limited for the radial direction by the uniform magnetic field applied in the axial direction. The electron trapped in the axial direction by the well shaped potential with negative barriers at both ends.

The experimental simulation of the pulse compression using the Malmberg-Penning trap device is performed by manipulating the barrier voltage to reduce the space between the potential barriers.

3. Numerical simulation model

Numerical simulations are performed under the experimental conditions as longitudinal compression process of HIB using the Malmberg-Penning trap device. In the numerical simulations, ten times compression from the initial condition, in which the compression ratio is 10, was carried out using the multi-particle simulation code [14], which represents a particle-particle model [15]. The particle position \mathbf{x}_i for i th super particle is calculated by

$$\frac{d}{dt}\mathbf{x}_i = \mathbf{v}_i \quad (1)$$

where the particle velocity \mathbf{v}_i for i th super particle is temporally changed by the external magnetic fields and the interaction with j th super particle. The particle velocity is calculated by Newton-Lorentz equation of motion

$$m \frac{d}{dt} \mathbf{v}_i = \frac{e^2}{4\pi\epsilon_0} \sum_{j \neq i}^N \frac{\mathbf{x}_i - \mathbf{x}_j}{(|\mathbf{x}_i - \mathbf{x}_j|^2 + s^2)^{3/2}} - e\mathbf{v}_i \times \mathbf{B}_{ext} \quad (2)$$

where m is the mass of electron, e is the elementary charge, ϵ_0 is the permittivity in vacuum, $\mathbf{B}_{ext} \equiv (0, 0, B_z)$ is the external magnetic flux density, s is the softening parameter, respectively.

At the initial condition, the electron number was set to be 1.6×10^8 with thermodynamic equilibrium distribution as 1 eV. The electrons were converted to 10000 super-particles that maintaining the mass-to-charge ratio and arranged uniformly in cylindrical space with 10 mm in radius and 180 mm in axial length. The boundary conditions at the both axial ends are set to be reflection boundary for the particles. The compression time and the external magnetic flux density are 100 ns and 0.01 T and 0.1 T, respectively.

4. Calculation results and Discussions

Figure 1 shows the charge density distribution in transverse real space for each external magnetic field density of 0.01 T and 0.1 T. The color map shows the normalized charge density logarithmic scale by the maximum value at each time. In comparison to the different strengths of the external magnetic field, the particles are confined by the potential barriers and the external magnetic field during the longitudinal compression in both cases. The results also show that the charge density distributions in both the strengths of external magnetic field are similar. From the initial condition, the Larmor radii estimated by the thermal velocity of 1 eV in the external magnetic field of 0.01 T and 0.1 T are 0.42 mm and 0.042 mm, respectively. In the case of weak external magnetic field as 0.01 T, the some particles deviate from the beam radius during the compression.

Figure 2 shows the normalized speed distribution in transverse space for each external magnetic field. At the initial condition, the normalized speed distribution in transverse fits with Maxwell distribution. As shown in Fig. 2, particles with higher velocity increase as the deviation from the Maxwell distribution for each external magnetic field. The rate of higher velocity particles in external

magnetic field of 0.01 T is higher than that in external magnetic density of 0.1 T. These results mean that the transverse velocity of the particles increase the longitudinal-transverse coupling of momentum due to the Coulomb interactions during the longitudinal compression.

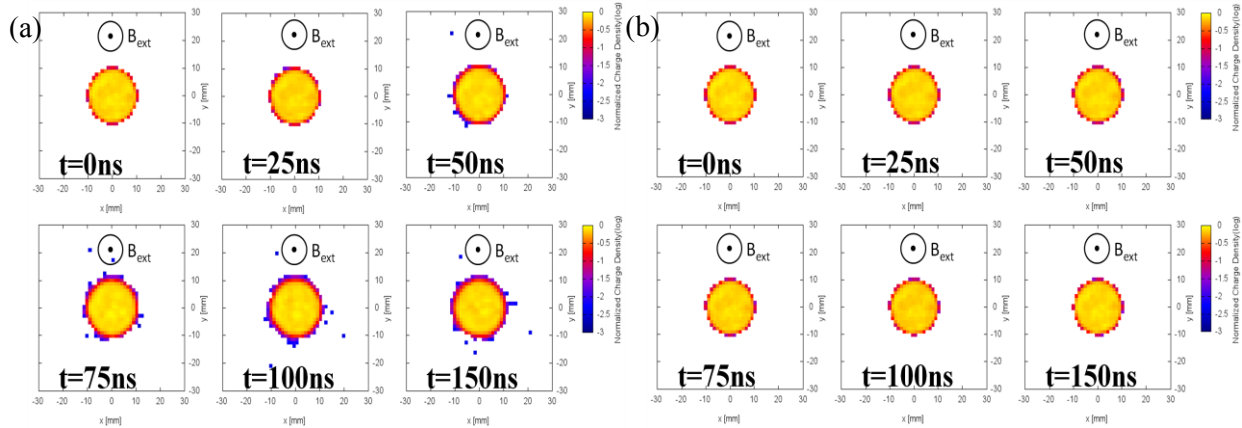


Figure 1. Normalized charge density distribution in transverse real space at each external magnetic flux density for (a) 0.01 T and (b) 0.1 T.

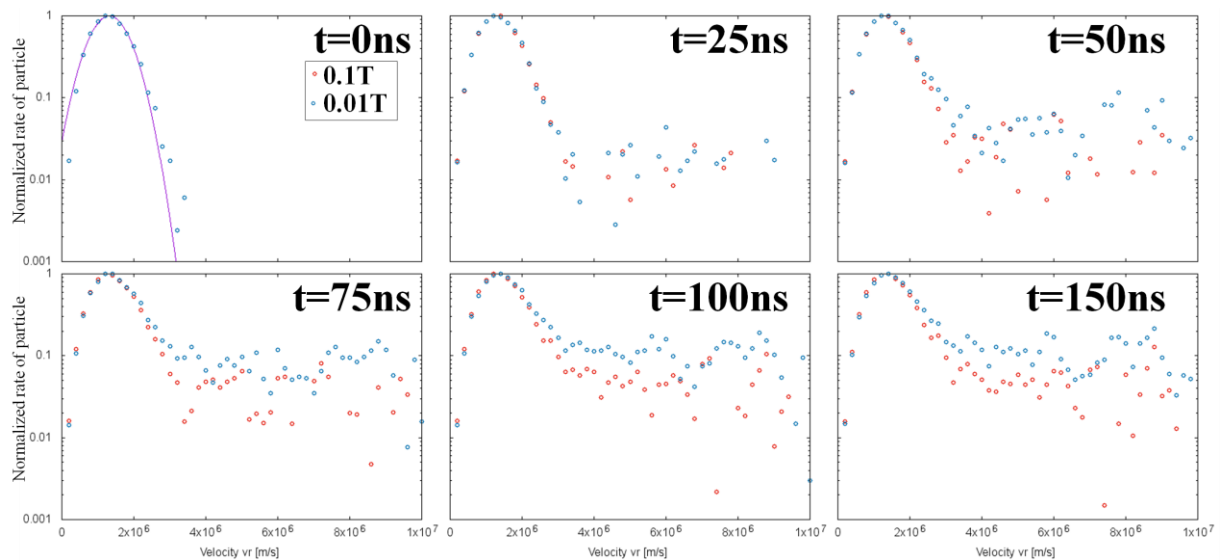


Figure 2. Normalized speed distributions in transverse direction at each external magnetic field.

Figure 3 shows the charge density distributions in the longitudinal phase space at the initial condition and at 150 ns for each external magnetic field density of 0.01 T and 0.1 T. The color map shows the normalized charge density logarithmic scale by the maximum value at each time. As shown in Fig. 3, the longitudinal velocity spread for both cases increase during the longitudinal compression. It should be noted that the longitudinal velocity distribution under the weak external magnetic field shows a larger spread in comparison to that under the strong external magnetic field. Therefore, the longitudinal velocity spread during the longitudinal compression depends on the external magnetic field.

From these results, both the transverse and longitudinal velocities increase during longitudinal compression for each external magnetic field. The Larmor radii estimated by the thermal velocity of 1 eV at each external magnetic field are considered to be negligible smaller than the beam radius. In other word, thermodynamic particle behavior is confined by the external magnetic field. However, the particles having high velocity have large Larmor radius in weak external magnetic field of 0.01 T. The some particles that deviate from the beam radius in the external magnetic field of 0.01 T would have

resulted by the Coulomb interaction during the longitudinal compression. This result suggests that the influence of space-charge effect depends on external magnetic field, as estimated by the tune depression, which is an index for space charge strength in the beam bunch [3].

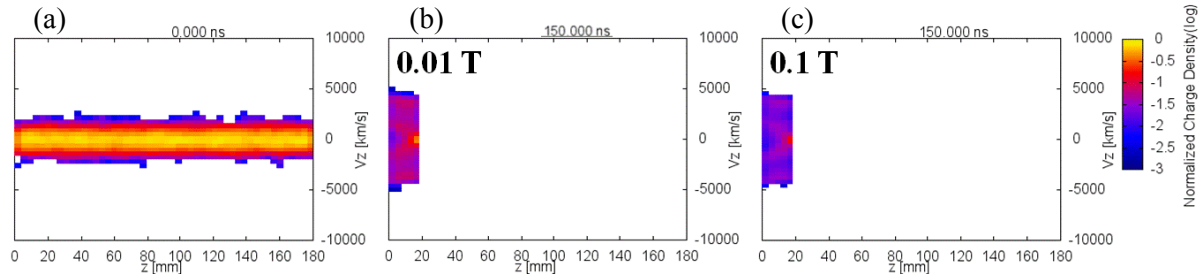


Figure 3. Normalized charge density in longitudinal phase space, (a) at initial condition, (b) 0.01 T, and (c) 0.1 T, after 250 ns in longitudinal pulse compression.

5. Conclusion

To simulate the pulse compression of space charge dominated beams for ICF driven by HIB, we have demonstrated the multi-particle numerical simulations as the equivalent beam dynamics using the Malmberg-Penning trap device. From the results of multi-particle numerical simulation for the compression process with different external magnetic fields, both the transverse and longitudinal velocities increase during longitudinal compression for each external magnetic field. In the weak external magnetic field as 0.01 T, some particles deviate from the beam radius during the longitudinal compression. The longitudinal velocity spread in the case of weak external magnetic field expands from the comparison of that in the case of strong external magnetic field. These mean that the space-charge effect influence depends on the external magnetic field.

In conclusion, the beam dynamics in Malmberg-Penning trap device has the influence of space-charge effect that depends on the external magnetic field. When thermodynamic particle behavior is confined by the external magnetic field, the influence of space-charge effect becomes strong in the case of weak external magnetic field.

References

- [1] Bangerter R O 1993 *il Nuovo Cimento* **106A** 1445
- [2] Prior C R 1998 *Proc. EPAC1998* 323
- [3] Yu S S *et al* 2003 *Fusion Science Tech.* **44** 266
- [4] Barnard J J *et al* 1998 *Nucl. Instrum. Methods Phys. Res. A* **415** 218
- [5] Kim C H *et al* 1986 *AIP Conf. Proc.* **152** 264
- [6] Ho D D M *et al* 1991 *Part. Accelerators* 35 15
- [7] Lee E P *et al* 2002 *Laser Part. Beams* **20** 581
- [8] De Hoon M J L *et al* 2003 *Phys. Plasmas* **10** 855
- [9] Qin H *et al* 2004 *Phys. Rev. STAB* **5** 034401
- [10] Sharp W M *et al* 2005 *Nucl Instrum Method Phys Res A* **544** 398
- [11] Park Y *et al* 2013 *NIFC PROC* **93** 84
- [12] Kikuchi T *et al* *in this conference*
- [13] Soga Y *et al* 2006 *Phys. Plasmas* **13** 052105
- [14] Kikuchi T *et al* 2015 *Progress in Nuclear Energy* 82 pp126-129
- [15] Hockney R W and Eastwood J W 1988 *Computer Simulation Using Particles* (Bristol and Philadelphia: IOP publishing)